Supplement of Atmos. Chem. Phys., 19, 2001–2013, 2019
https://doi.org/10.5194/acp-19-2001-2019-supplement

Atmospheric Chemistry and Physics
Open Access
EGU

Supplement of

Rate constant and secondary organic aerosol formation from the gas-phase reaction of eugenol with hydroxyl radicals

Changgeng Liu et al.

Correspondence to: Yongchun Liu (liuyc@buct.edu.cn) and Hong He (honghe@rcees.ac.cn)

1. Experimental details

OH radical reactions were performed in an oxidation flow reactor (OFR) consisting of two electro-polished stainless steel cylinders, i.e., the static mixing tube (29.3 cm (length)) and the reaction chamber (7.3 cm (inner diameter) × 25 cm (length)). Before entering into the reaction chamber, gas-phase species were mixed sufficiently in the mixing tube. Fluid dynamics simulations of mixing tube confirmed that gas-phase species were well mixed with a uniform initial velocity profile. The average reaction time of OH with eugenol was 26.7 s calculated from the illuminated volume (0.89 L) and the total flow rate (2 L min^{-1}). The temperature of the reactor was maintained at 301 K by circulating water through the outer jacket of the OFR.

Liquid pure eugenol placed in a brown bubbler was gently heated and the carrier gas (zero air) brought gas-phase eugenol into the OFR. The concentrations of gas-phase eugenol in the OFR were controlled by the flow rate of carrier gas. Similarly, gas-phase reference compound (*m*-xylene and 1,3,5-trimethylbenzene) was also introduced into the OFR via a brown bubbler without heating. The concentrations of gas-phase species were determined by a commercial high-resolution proton-transfer reaction time-of-flight mass spectrometer (HR-PTR-QiToF-MS) (Ionicon Analytik GmbH). The concentration of eugenol was calibrated by a commercial permeation tube (VICI AG INTERNATIONAL Valco Instruments Co., Inc.). The toolkit Squirrel 1.16H was used to analyze the mass concentrations of sulfate, nitrate, and organics, measured by an Aerodyne high-resolution time-of-flight aerosol mass spectrometer (HR-ToF-AMS).

NO_2 concentration was determined by a NO_x analyzer (Model 42i-TL, Thermo Fisher Scientific Inc.).

Before photochemical reaction, the concentration of O_3 in the OFR was in the range of 0.94−9.11 ppmv, which decreased to 0.39−6.02 ppmv due to the consumption by H_2O with 254 nm UV light. In order to evaluate the possible decay of eugenol via the reaction with O_3 and the possible SOA formation from their reaction, the control experiments were conducted in this work. The results showed that the concentration of eugenol was not affected by O_3 and no SOA formation was observed by SMPS and HR-ToF-AMS. In addition, the possible effects of O_3 on the decay of reference compounds (i.e., 1,3,5-trimethylbenzene and *m*-xylene) were also investigated. The results showed that the decays of reference compounds by O_3 could be ignored in this work. The variations in the concentrations of eugenol and reference compounds (i.e., 1,3,5-trimethylbenzene and *m*-xylene) in the presence of 9.11 ppmv O_3 are shown in Fig. S3. These results were mainly resulted from the short reaction time in the OFR and the low rate constants of O_3 with methoxyphenols (~10^{-19} cm^3 $molecule^{-1}$ s^{-1}) (El Zein et al., 2015) and reference compounds (~10^{-21} cm^3 $molecule^{-1}$ s^{-1}) (Atkinson et al., 1982; Yu et al., 2012). The concentrations of OH radicals were measured using SO_2 as the reference compound in a manner described previously (Lambe et al., 2015; Zhang et al., 2017). Approximately 200 ppbv SO_2 was introduced into the OFR by mass flow controller (MFC). Control experiments showed that SO_2 concentration was not affected individually by vapor H_2O, O_3, and 254 nm UV light. OH exposure ([OH]t) was

59 determined from the measured fractional loss of SO_2, $[SO_2]/[SO_2]_0$.

60 $$[OH]t = -\frac{1}{k_{SO_2}} \ln \frac{[SO_2]}{[SO_2]_0} \quad \text{(S1)}$$

61 where k_{SO_2} is the second-order rate consant of SO_2 with OH radicals at 298 K (9×10^{-13}

62 cm^3 $molecule^{-1}$ s^{-1}) (Davis et al., 1979).

63 Eugenol (Sigma-Aldrich, 99%), 1,3,5-trimethylbenzene (Sigma-Aldrich, 99.8%),

64 and *m*-xylene (Sigma-Aldrich, 99.5%) were used in the experiments as received. NO_2

65 (105 ppmv) and SO_2 (100 ppmv) were from Beijing Huayuan Gas Chemical Industry

66 Co., Ltd.

67 **2. Calculation of organic nitrate fraction**

68 The fraction of organic nitrate can be typically calculated according to the following

69 equation (Fry et al., 2013):

70 $$RONO_{2,frac} = \frac{(R_{experiment} - R_{NH_4NO_3})(1 + R_{RONO_2})}{(R_{RONO_2} - R_{NH_4NO_3})(1 + R_{experiment})} \quad \text{(S2)}$$

71 where $RONO_{2,frac}$ is the fraction of organic nitrate, $R_{experiment}$ is the ratio of

72 NO_2^+ / NO^+ measured by HR-ToF-AMS in the experiments, $R_{NH_4NO_3}$ (0.295) and

73 R_{RONO_2} (0.13) are the NO_2^+ / NO^+ ratios for ammonium nitrate and organic nitrates,

74 respectively (Fry et al., 2013).

75 **3. Calculation of OH suppression**

76 The OH suppression by external OH reactivity in the OFR is estimated according to the

77 OFR exposure estimator (v2.3) developed by Jimenez's group based on the estimation

78 equations reported in the previous work (Li et al., 2015; Peng et al., 2015, 2016). The

concentration of O_3 required by this estimator is in the range of 7−70 ppmv. Thus, O_3 with the concentrations of 7.8 and 9.1 ppmv in this work was used for this estimator. In addition, RH and rate constant for eugenol with OH radicals were 44% and 8.01×10^{-11} cm^3 $molecule^{-1}$ s^{-1} used in this estimator. The external OH reactivity in this estimator was only taken eugenol into account, due to its much higher concentration than those of SO_2 and NO_2. The external OH reactivity was calculated to be in the range of 85 s^{-1} to 410 s^{-1}, according to the following equation (Peng et al., 2015):

$$OHR_{ext} = k_{eugenol+OH}[eugenol] \quad (S3)$$

where OHR_{ext} is the external OH reactivity, $k_{eugenol+OH}$ is the rate constant of eugenol with OH radicals, and $[eugenol]$ is the concentration of eugenol.

According to the parameters mentioned above, the maximum reduction of OH exposure by eugenol in the OFR was approximately 90%.

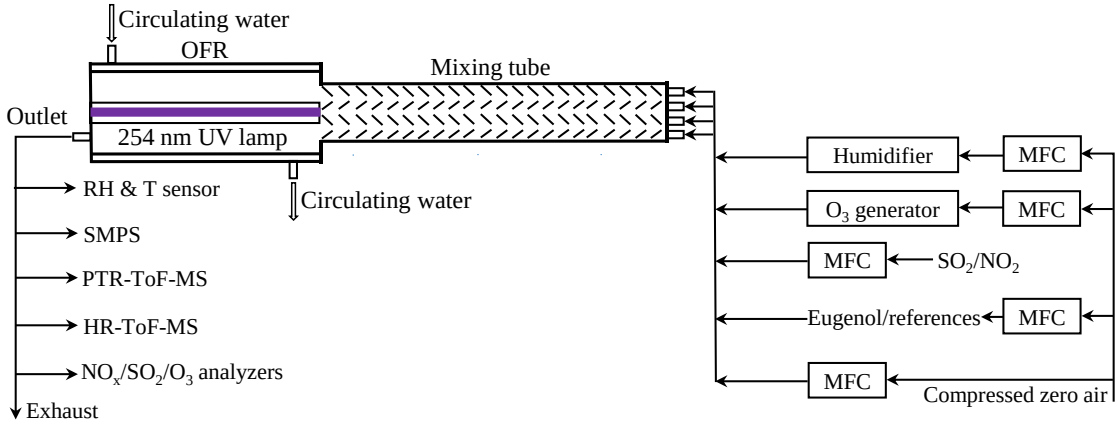

91

92 **Figure S1.** Experimental system used in this work.

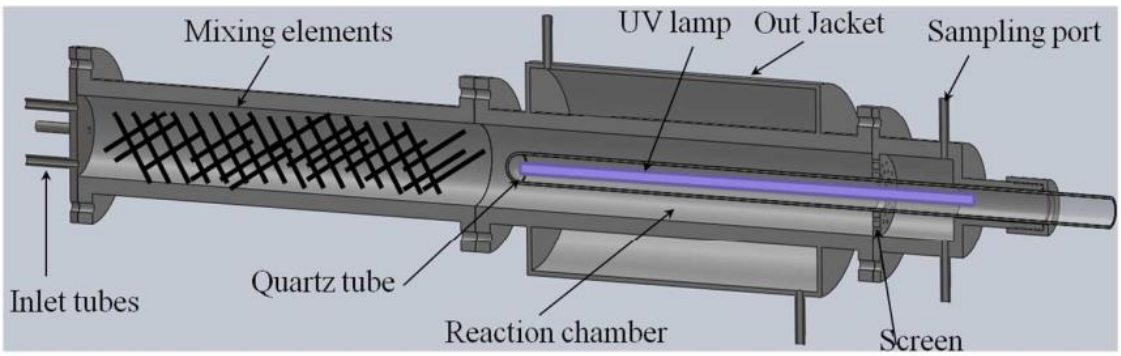

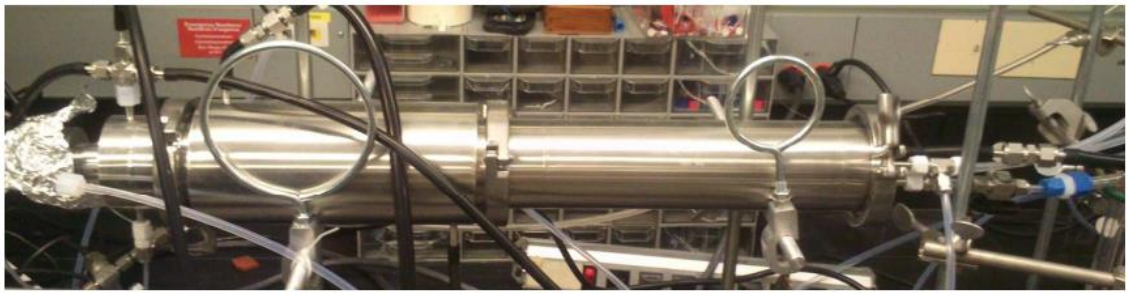

93

94 **Figure S2.** Detailed view of the Flow Oxidation Reactor and a photo of the reaction

95 system.

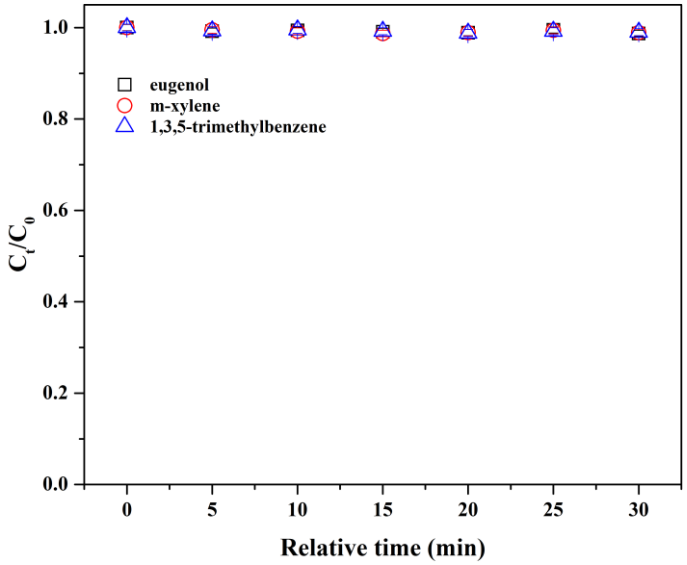

Figure S3. Variations in the concentrations of eugenol and reference compounds (i.e., 1,3,5-trimethylbenzene and *m*-xylene) in the presence of 9.11 ppmv O_3.

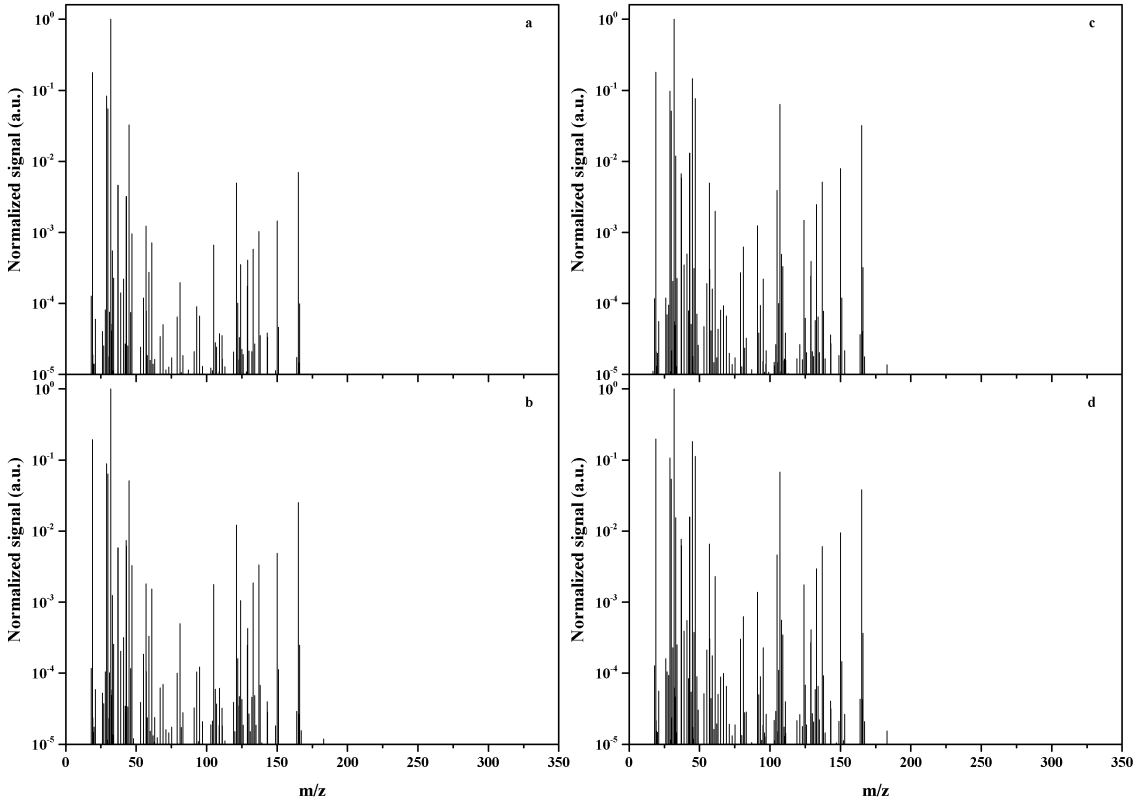

Figure S4. Normalized mass spectra of the gas mixtures of eugenol and 1,3,5-trimethylbenzene in the dark (a) and light (b), as well as eugenol and *m*-xylene in the dark (c) and light (d).

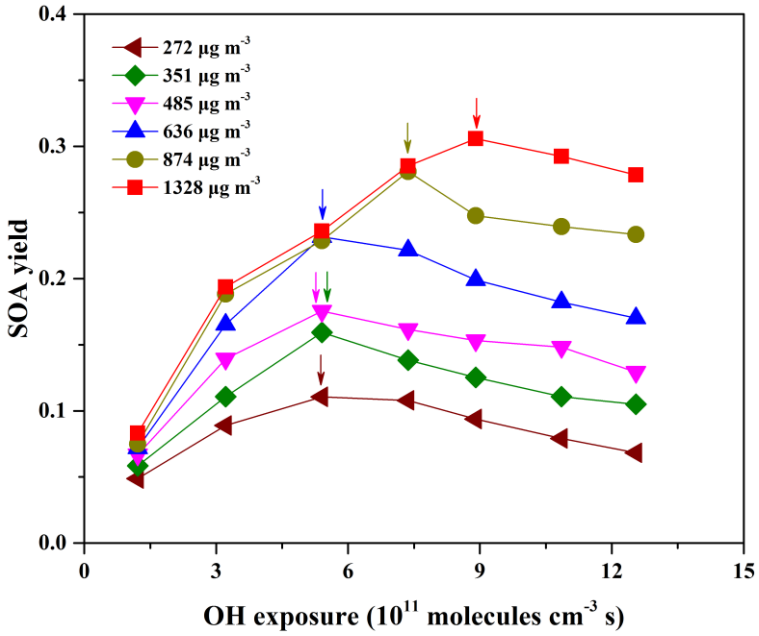

103

104 **Figure S5.** SOA yield vs. OH exposure for SOA formed from different eugenol

105 concentrations. The arrows indicate the maximum values (i.e., those listed in Table 2).

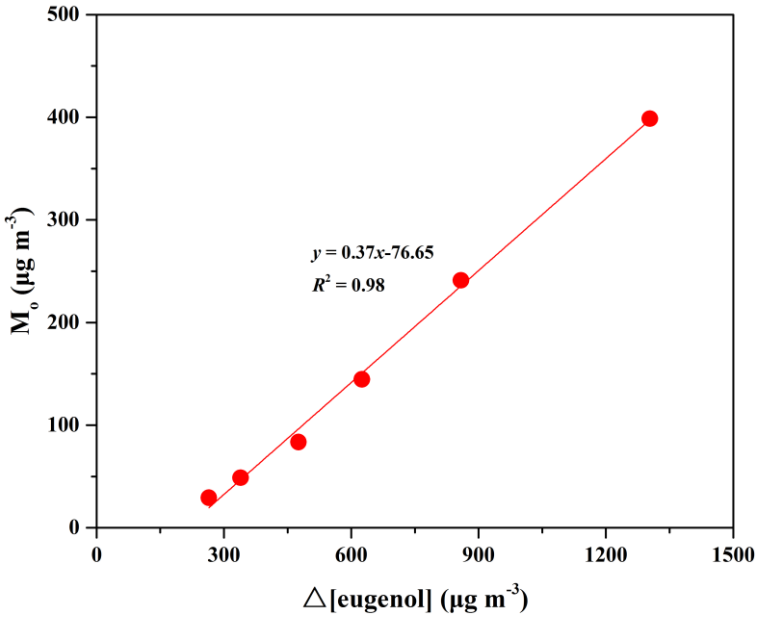

106

107 **Figure S6.** SOA mass concentration (M_o) vs. consumed eugenol concentration

108 (△[eugenol]). Each data point represents a separate experiment.

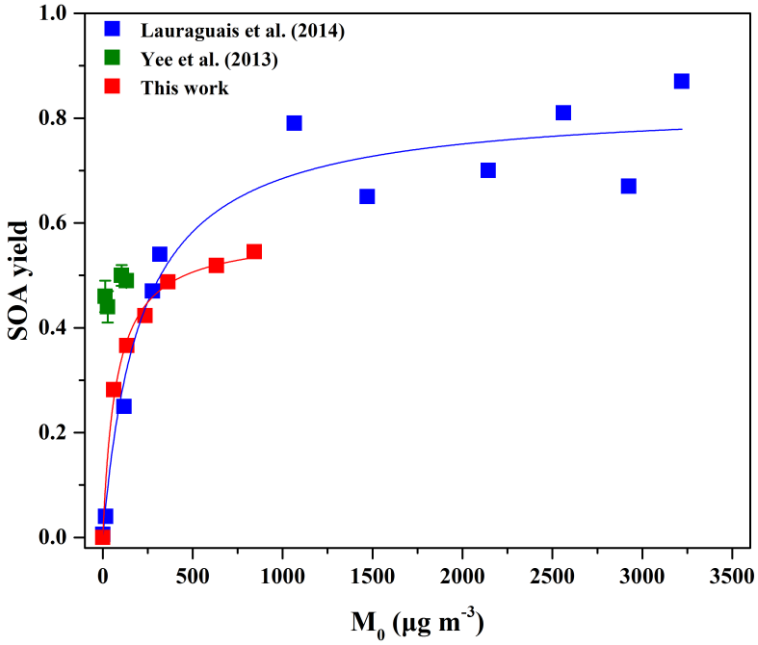

Figure S7. SOA yield as a function of SOA mass concentration (M_0) formed from the OH reactions at different guaiacol concentrations. The solid lines were fit to the experimental data using a one-product model. Values of α and $K_{om,i}$ used to generate the solid line are (0.58 ± 0.02) and (0.014 ± 0.001) in this work, and their values are (0.83 ± 0.04) and (0.005 ± 0.001) for the blue data from Lauraguais et al.(2014). The olive data are obtained from Yee et al. (2013).

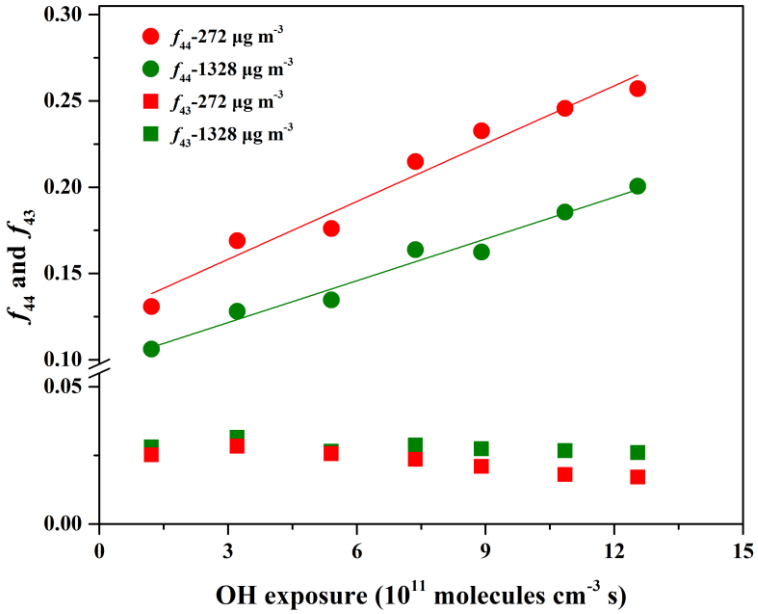

116

117 **Figure S8.** f_{44} and f_{43} vs. OH exposure for SOA formed at two eugenol concentrations

118 (272 and 1328 μg m^{-3}).

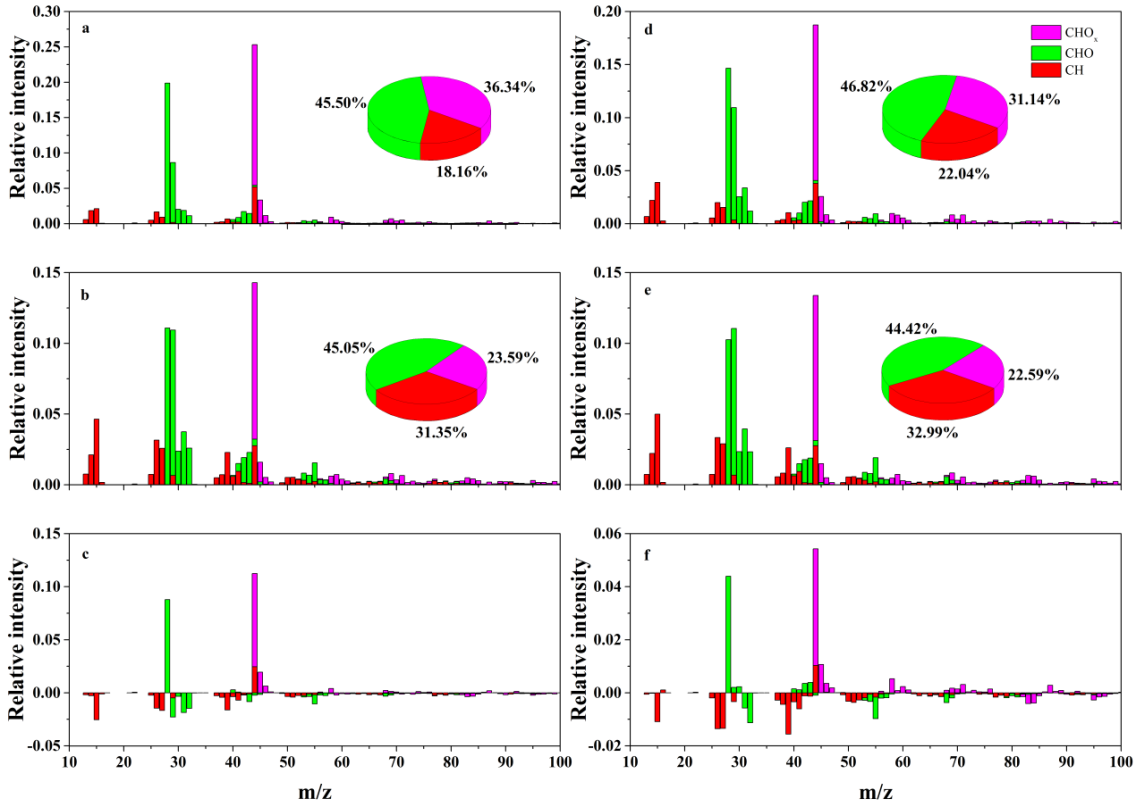

Figure S9. (a and d) Mass spectra of SOA at OH exposure of 12.55×10^{11} molecules s^{-1}. (b and e) Mass spectra of SOA at OH exposure of 1.21×10^{11} molecules s^{-1}. (c) Difference in mass spectra between (a) and (b). (f) Difference in mass spectra between (d) and (e). The data of (a-c) and (d-f) were taken from the aging processes of eugenol at two concentrations of 272 and 1328 μg m^{-3}, respectively.

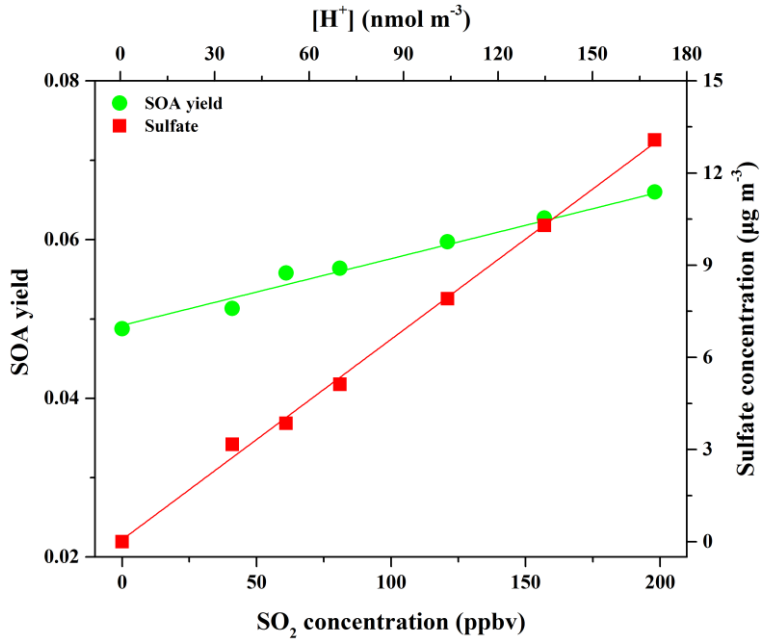

125

126 **Figure S10.** Effects of SO_2 concentration on SOA yield and sulfate formation in the

127 reaction of eugneol with OH radicals at OH exposure and eugenol concentration of 1.21

128 $\times 10^{11}$ molecules cm^{-3} s and 264 μg m^{-3}, respectively. The in situ particle acidity was

129 calculated as H^+ concentrations ($[H^+]$) according to the AIM-II model for

130 $H^+ - NH_4^+ - SO_4^{2-} - NO_3^- - H_2O$ system.

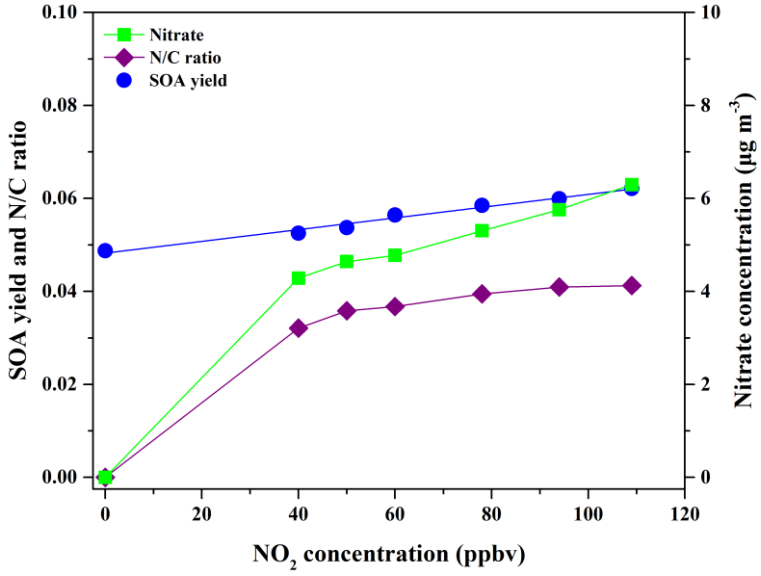

131

132 **Figure S11.** Evolution of SOA yield, nitrate formation, and N/C ratio as a function of

133 NO_2 concentration at OH exposure and eugenol concentration of 1.21×10^{11} molecules

134 cm^{-3} s and 268 μg m^{-3}, respectively.

References

Atkinson, R., Aschmann, S. M., Fitz, D. R., Winer, A. M., Pitts, J. N.: Rate constant for the gas-phase reactions of O_3 with selected organics at 296 K, Int. J. Chem. Kinet. 14, 13-18, doi: 10.1002/kin.550140103, 1982.

Davis, D.D., Ravishankara, A.R., Fischer, S.: SO_2 oxidation via the hydroxyl radical: Atmospheric fate of HSO_x radicals, Geophys. Res. Lett., 6, 113-116, doi: 10.1029/GL006i002p00113, 1979.

El Zein, A., Coeur, C., Obeid, E., Lauraguais, A., Fagniez, T.: Reaction kinetics of catechol (1,2-benzenediol) and guaiacol (2-methoxyphenol) with ozone, J. Phys. Chem. A 119, 6759-6765, doi: 10.1016/j.atmosenv.2013.11.074, 2015.

Fry, J. L., Draper, D. C., Zarzana, K. J., Campuzano-Jost, P., Day, D. A., Jimenez, J. L., Brown, S. S., Cohen, R. C., Kaser, L., Hansel, A., Cappellin, L., Karl, T., Hodzic Roux, A., Turnipseed, A., Cantrell, C., Lefer, B. L., and Grossberg, N.: Observations of gas- and aerosol-phase organic nitrates at BEACHON-RoMBAS 2011, Atmos. Chem. Phys., 13, 8585-8605, 10.5194/acp-13-8585-2013, 2013.

Lambe, A.T., Chhabra, P.S., Onasch, T.B., Brune, W.H., Hunter, J.F., Kroll, J.H., Cummings, M.J., Brogan, J.F., Parmar, Y., Worsnop, D.R., Kolb, C.E., Davidovits, P.: Effect of oxidant concentration, exposure time, and seed particles on secondary organic aerosol chemical composition and yield, Atmos. Chem. Phys., 15, 3063-3075, doi: 10.5194/acp-15-3063-2015, 2015.

Lauraguais, A., Coeur-Tourneur, C., Cassez, A., Deboudt, K., Fourmentin, M., Choel,

M.: Atmospheric reactivity of hydroxyl radicals with guaiacol (2-methoxyphenol), a biomass burning emitted compound: Secondary organic aerosol formation and gas-phase oxidation products, Atmos. Environ., 86, 155-163, doi: 10.1016/j.atmosenv.2013.11.074, 2014.

Li, R., Palm, B. B., Ortega, A. M., Hlywiak, J., Hu, W., Peng, Z., Day, D. A., Knote, C., Brune, W. H., de Gouw, J. A., and Jimenez, J. L.: Modeling the radical chemistry in an oxidation flow reactor: Radical formation and recycling, sensitivities, and the OH exposure estimation equation, J. Phys. Chem. A, 119, 4418-4432, doi: 10.1021/jp509534k, 2015.

Peng, Z., Day, D. A., Stark, H., Li, R., Lee-Taylor, J., Palm, B. B., Brune, W. H., and Jimenez, J. L.: HOx radical chemistry in oxidation flow reactors with low-pressure mercury lamps systematically examined by modeling, Atmos. Measur. Tech., 8, 4863-4890, 10.5194/amt-8-4863-2015, 2015.

Peng, Z., Day, D. A., Ortega, A. M., Palm, B. B., Hu, W., Stark, H., Li, R., Tsigaridis, K., Brune, W. H., and Jimenez, J. L.: Non-OH chemistry in oxidation flow reactors for the study of atmospheric chemistry systematically examined by modeling, Atmos. Chem. Phys., 16, 4283-4305, doi: 10.5194/acp-16-4283-2016, 2016.

Yee, L.D., Kautzman, K.E., Loza, C.L., Schilling, K.A., Coggon, M.M., Chhabra, P.S., Chan, M.N., Chan, A.W.H., Hersey, S.P., Crounse, J.D., Wennberg, P.O., Flagan, R.C., Seinfeld, J.H.: Secondary organic aerosol formation from biomass burning intermediates: Phenol and methoxyphenols, Atmos. Chem. Phys., 13, 8019-8043,

177 doi: 10.5194/acp-13-8019-2013, 2013.

178 Yu, X., Yi, B., Wang, X., Chen, J.: Predicting reaction rate constants of ozone with
179 organic compounds from radical structures, Atmos. Environ. 51, 124-130, doi:
180 10.1016/j.atmosenv.2012.01.037, 2012.

181 Zhang, X., Lambe, A. T., Upshur, M. A., Brooks, W. A., Be, A. G., Thomson, R. J.,
182 Geiger, F. M., Surratt, J. D., Zhang, Z.; Gold, A., Graf, S., Cubison, M. J., Groessl,
183 M., Jayne, J. T., Worsnop, D. R., Canagaratna, M. R.: Highly oxygenated
184 multifunctional compounds in alpha-pinene secondary organic aerosol, Environ.
185 Sci. Technol. 51, 5932-5940, doi: 10.1021/acs.est.6b06588, 2017.